Research Article

Chengyang Xu, Xueqing Liu, Fujia Li, Heguo Fu, Dong Han, Ning Huang, Gongdong Wang*, and Yiwen Wang

Wear mechanism analysis of internal chip removal drill for CFRP drilling

https://doi.org/10.1515/secm-2024-0013
received May 22, 2023; accepted April 16, 2024

Abstract: As one of the main problems in the processing of carbon fiber reinforced polymer (CFRP), tool wear affects the quality and efficiency of hole making. As a new CFRP hole making process, the suction-type internal chip removal method can effectively slow down the tool wear rate. In order to further clarify the reasons for this method to slow down the tool wear, this study investigates the wear mechanism of the internal chip removal tool. The main contents include: first, the experimental parameters such as drilling axial force, drilling temperature, and tool wear are obtained through the experimental method, and the drawing of the drilling temperature change curve of internal chip drilling is completed; second, the polar analysis method is used to study the influence of the drill parameters on the drilling axial force and the tool wear, and the basis for the selection of the structure of the internal chip drill is given; finally, the method of comparative experiments of the internal chip drilling process and the non-internal chip drilling process is used to conclude that the use of the internal chip drilling process can effectively slow down the tool wear rate. Finally, the method of comparing the internal chip removal and non-internal chip removal processes is used to conclude that the use of internal chip removal processing method can effectively reduce the axial force, drilling temperature, and slow down the tool wear.

Keywords: CFRP, hole making, suction-type internal chip removal machining method, wear mechanism, internal chip removal tool

*** Corresponding author: Gongdong Wang,** College of Aerospace Engineering, Shenyang Aerospace University, Shenyang, 110136, China, e-mail: cadcam119@126.com
Chengyang Xu: College of Aerospace Engineering, Shenyang Aerospace University, Shenyang, 110136, China; Key Laboratory of Advanced Manufacturing and Intelligent Technology (Ministry of Education), Harbin, 150080, China, e-mail: Xuchengyang199101@163.com
Xueqing Liu: College of Aerospace Engineering, Shenyang Aerospace University, Shenyang, 110136, China
Fujia Li, **Heguo Fu**, **Dong Han**, **Ning Huang:** Shenyang Aircraft Corporation, Shenyang, 110136, China
Yiwen Wang: Key Laboratory of Advanced Manufacturing and Intelligent Technology (Ministry of Education), Harbin, 150080, China

1 Introduction

Carbon fiber reinforced polymer (CFRP) is widely used in aerospace, automotive, and other fields for excellent physical and mechanical properties in many lightweight materials [1]. The rapid tool wear in CFRP hole- machining is one of the problems that needs to be solved. Suction type internal chip removal machining method can realistically remove the chips generated during the cutting process through the tool interior during the drilling process, which has been found to effectively reduce the wear speed of the tool [2]. The machining mechanism, tool wear law, and failure form of CFRP drilling process are studied and analyzed.

Due to the special characteristics of CFRP material itself and the high hardness and high wear resistance of the carbon fiber reinforced phase, it causes a strong frictional effect between the carbon-fiber-based hard points and the cutting edge of the drill bit during the cutting process, resulting in rapid wear of the drill bit [3]. In order to effectively reduce tool wear, reduce machining defects, and improve hole-machining quality, the form and mechanism of CFRP tool wear need to be investigated, at the earliest. Teti [4], through experimental studies of tool wear, concluded that the mechanical form of hard point wear is the most important form of wear for CFRP drilling tools. Rawat and Attia [5], by studying the wear of carbide drills machining CFRP, concluded that the main wear mechanism of the tool is the scraping effect of hard point particles on the cutting edge of the drill and the chipping phenomenon caused by the destruction of the binder cobalt (Co) in the carbide drill. Mayuet *et al.* [6] used an energy-dispersive spectrometer (EDS) to perform elemental analysis of drill wear after drilling CFRP and found that the tool wear contained a large amount of carbon elements and a small amount of binder (Co) elements, indicating that chemical

forms of wear such as bonding and diffusion occur when drilling CFRP. However, Wang *et al.* and Karpat *et al.* [7,8] found that during CFRP drilling, the drilling temperature is not very high and chemical forms of wear generally rarely occur; therefore, bonded and diffuse wear are not among the main wear mechanisms of CFRP tools. Çelik *et al.* and Ramirez *et al.* [9,10] conducted an experimental study on the wear of CFRP drilling tools with carbide-coated drill bits and concluded that the main forms of tool wear are blunting of the cutting edge, chipping of the edge, wear of the rear tool face and micro chipping of the coating. Also, Xia *et al.* [11] found that, in addition to the wear of the main cutting edge and the rear tool face, the edge band of the drill bit also shows wear. In order to solve the problem of tool wear seriously affecting the machining surface quality, exacerbating burrs, tearing, delamination and other hole defects unique to composite materials, most scholars have basically studied the material, structure, and machining process of the tools. Bao and Gao *et al.* [12,13] developed a "grinding instead of drilling" electroplated diamond drilling and grinding combination tool. The combination tool can effectively reduce the wear rate and improve the tool life and machining efficiency. Zhao *et al.* Peng *et al.* and Wei [14–16] studied the tool wear of coated, uncoated carbide twist drills and polycrystalline diamond (PCD) inlay drills when machining CFRP by experimental methods, and found that the hard points at the corner of the outer edge of the main cutting edge of uncoated carbide twist drills were the most severely worn; the tool wear of coated carbide twist drills was mainly due to the spalling of the coating, micro chipping of the cutting edge and carbon fiber. The wear of PCD inlay drill is mainly mechanical wear and chip and resin adhesion wear. Qian *et al.* and Wang *et al.* [17–19] studied the wear of the cross edge and the second main cutting edge by internal coolant holes double point angle drill, and found that the reverse cooling process could reduce the drilling temperature and inhibit the tool wear by opening the internal coolant holes on the cutting edge and using the micro-cooling lubrication process. To improve the hole-machining quality and tool life of drilling CFRP/Ti laminated composites, Yang *et al.* and Li *et al.* [20,21] proposed a low-frequency vibration-assisted drilling (LFVAD) process, and by comparing the tool wear analysis with that of ordinary drilling, it was found that the total wear of LFVAD drills was small and the wear distribution was uniform, which could effectively improve the machining quality.

In summary, it can be seen that scholars have conducted experimental studies on CFRP tool wear using different processes for different materials and special structures of drills, and concluded that the tool wear mechanisms and failure forms are different for different machining processes and different tool structures. Also, it is found that the reverse cooling process can achieve the effect of reducing drilling temperature and inhibiting tool wear. Therefore, this work studies the wear mechanism of internal chip drilling tools under the internal chip processing, and provides a theoretical research basis for the subsequent optimization of the internal chip processing and internal chip tools.

2 Experimental conditions

2.1 Experimental conditions for CFRP internal chip removal drilling process

2.1.1 Workpiece materials and parameters

The workpiece material selected for the experiment is a T800-grade CFRP laminate. Of these, carbon fiber has a volume ratio of 65%. The thickness is 4.96 mm and the material size is 21 mm × 20.5 mm, as shown in Figure 1. The mechanical performance parameters of CFRP laminates are shown in Table 1.

In the table, $\boldsymbol{E}_1$ is the elastic modulus in the X direction; $\boldsymbol{E}_2$ is the elastic modulus in the Y direction; $\boldsymbol{G}_{12}$ is the shear modulus of the XOY plane; $\boldsymbol{v}_{12}$ is the Poisson's ratio; ρ is the density; $\boldsymbol{X}^{\mathrm{T}}$ is the X direction tensile strength; $\boldsymbol{X}^{\mathrm{C}}$ is the X direction compression strength; $\boldsymbol{Y}^{\mathrm{T}}$ is the Y direction tensile

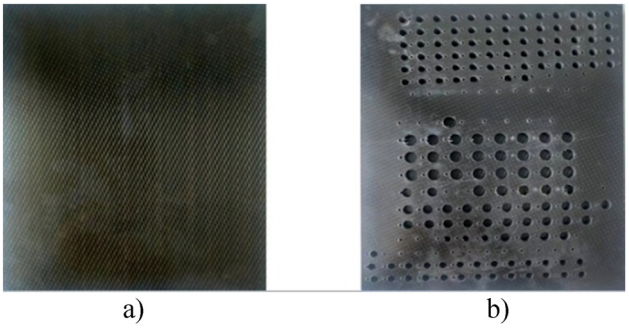

Figure 1: CFRP workpiece materials. (a) Before machining and (b) after machining.

Table 1: CFRP mechanical performance parameters

$\boldsymbol{E}_1$ (GPa)	$\boldsymbol{E}_2$ (GPa)	$\boldsymbol{G}_{12}$ (GPa)	$\boldsymbol{v}_{12}$	$\boldsymbol{P}$ (kg/m^3)
230	14	28	0.3	1,760
$\boldsymbol{X}^{\mathrm{T}}$ (MPa)	$\boldsymbol{X}^{\mathrm{C}}$ (MPa)	$\boldsymbol{Y}^{\mathrm{T}}$ (MPa)	$\boldsymbol{Y}^{\mathrm{C}}$ (MPa)	$\boldsymbol{S}$ (MPa)
3,530	1,800	350	2,730	380

strength; Y^C is the Y direction compression strength; and S is the shear strength.

The drill bit used in the experiment was provided by Guohong Tool System (Wuxi) Co., Ltd as shown in Figure 2. The carbide drill bits with inner chip drains function (the diameter of the inner chip channel is 2 mm) and the carbide drill bits without inner drains, respectively, the geometric parameters of the drill bit are shown in Table 2.

2.2 Experimental platform for drilling of inner chip

The suction-type internal chip removal system (Figure 3) for experiment is composed of machine tool, CFRP, external-rotation-internal-chip removal tool handle, inner-chip-removal drilling bit, chip pipe, chip collecting device, and so on. Among them, the internal chip removal drilling bit and the external-rotation-internal-chip-removal tool handle had chip removal holes.

The function of the system is to discharge the chips generated in the drilling process of CFRP in real time through the chip removal channel, reduce the cost of manpower and material resources, improve the efficiency and quality of drilling, and realize the green processing of CFRP. The working principle of the system is that, when the machine tool is working, the spindle drives the suction type inner-chip-removal drilling bit installed on the external and external-rotation-internal-chip removal tool handle to drill. At the same time, the fan in the chip collecting device

Figure 2: Carbide drill bits.

Table 2: Geometric parameters of the drill bit

Drill Type	Drill material	Helix angle (°)	Drill diameter (mm)	Point angle (°)	Rear angle (°)
Straight shank twist drill	YG6X	30	6	90	8
			8	110	12
			9	120	16
			10	140	20

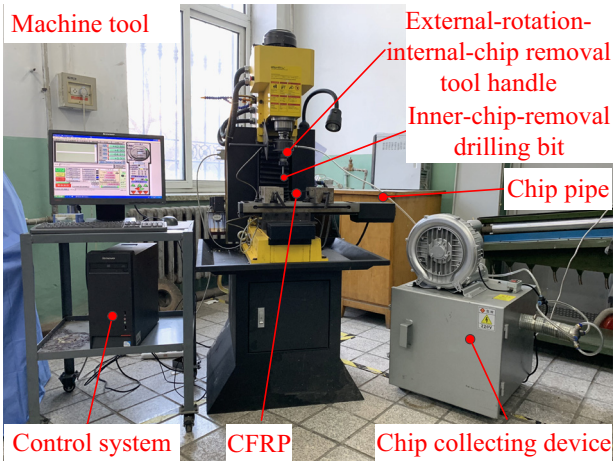

Figure 3: Suction-type internal chip removal system.

provides the power to absorb chips (negative pressure), the system uses the negative pressure to suck chips out through the chips suction channel of the drill bit, and sucks the chips through the chip removal channel of the drill bit and the external-rotation-internal-chip removal tool handle with the chips removal channel into the chip collecting device, thus completing the process of the aspiration-type internal chips removal drilling.

2.3 Data acquisition and workpiece inspection device

The internal chip removal experiment is carried out on a KV800 CNC milling machine (Figure 4), where the axial force is collected by the Kistler 9257B three-way dynamic piezoelectric dynamometer, transmitted to the data acquisition system *via* the Kistler 5070A charge amplifier, and output by the DHDAS test system software.

The drilling heat is measured by means of pre-buried thermocouple, and the temperature measurement system consists of *K*-type thermocouple and data collecting instrument, as shown in Figure 5. Before the experiment, a 2 mm diameter hole needs to be drilled at a suitable location on the CFRP workpiece to pre-bury the thermocouple, at a depth of about 3 mm from the surface. The distance between the experimental hole and the buried wire hole is 1 mm (Figure 6a), and the actual diagram of the distance between the pre-buried thermocouple hole and the experimental hole is shown in Figure 6b. During the drilling process, the temperature change value measured by the thermocouple was displayed by the data collecting instrument, and the highest temperature during the drilling process was selected as the drilling temperature in this study. In addition, an

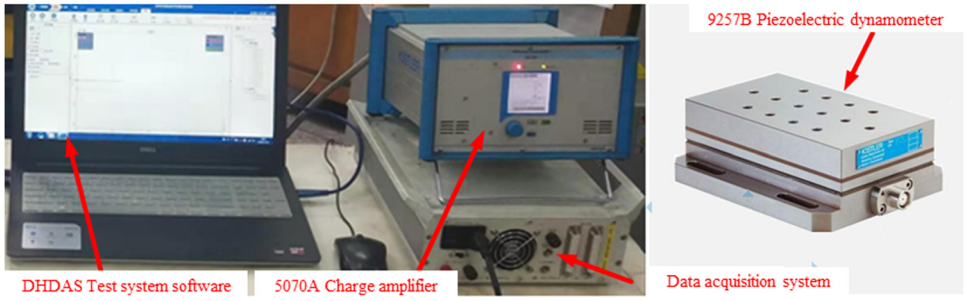

Figure 4: Drilling axial force acquisition system.

Figure 5: Temperature measurement system. (a) *K*-type thermocouple and (b) data collecting instrument.

ultra-depth-of-field microscope (VHX-1000) from Keenes was used for tool wear inspection.

2.4 Orthogonal experimental design and data collection

Axial force is the main factor leading to CFRP hole-machining defects (delamination, tearing), and the study of the change law of axial force and tool wear will be beneficial to reduce hole-machining defects and improve machining quality. When drilling CFRP, as the amount of tool wear increases, the cutting edge of the drill becomes increasingly blunt, making it more and more difficult for the tool to remove the material. When the tool wear value reaches a certain level and the drill bit is worn out and no longer has good cutting performance, the axial force will also change dramatically. To study the factors affecting tool wear, a large number of experiments need to be conducted, which is time-consuming. In order to derive the influencing factors related to tool wear more quickly and accurately, this work conducts a study on internal chip removal tool wear by designing orthogonal experiments.

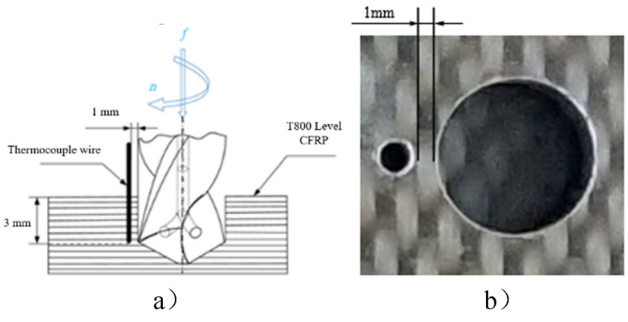

Figure 6: Thermocouple pre-buried location. (a) Thermocouple buried wire. (b) Hole spacing measurement.

2.4.1 Orthogonal experimental design and protocol

For the purpose of wear study, this work selects carbide twist drill for machining T800 CFRP, and reasonable guidelines for tool selection by studying the change law of axial force, drilling temperature, and tool wear is given.

Cutting parameters: spindle speed was 3,000 rpm, feed rate was 20 mm/min, and the drill bit was the same batch of the same manufacturer. A three-factor, four-level orthogonal experiment was designed to study the variation in the axial force and tool wear under different drill parameters, and the factor level table is shown in Table 3. In order to truly reflect the changes between axial force, drilling temperature, and tool wear under different drill parameters, the axial force and drilling temperature were measured for each hole, and the tool wear was measured once every five holes processed.

Table 3: Factor level table

	Drill diameter/(mm)	Point angle/(°)	Rear angle/(°)
1	6	90	8
2	8	110	12
3	9	120	16
4	10	140	20

2.4.2 Experimental data collection and result analysis

During the drilling process, the axial force and drilling temperature during the drilling process were measured in real time by the force measurement system and temperature measurement system, and the tool wear of the drill bit was measured by the ultra-depth-of-field microscope, and the collected experimental data are shown in Table 4.

It can be seen from the experimental data in Table 4 that the maximum value of axial force is 123.6 N and the minimum value is 90.8 N; the maximum value of drilling temperature is 117°C and the minimum value is 94.°C; the maximum value of chisel edge width is 45 μm and the minimum value is 30 μm; the maximum value of rounded CER is 57.46 μm and the minimum value is 33.31 μm; and the maximum value of flank wear land width is 252 μm and the minimum value is 177 μm. From the overall point of view, the variation intervals of axial force, drilling temperature, and tool wear values are large, which indicates that changing the drill parameters has a certain influence on the drilling process.

2.4.3 Study of the variation process of drilling temperature

During the drilling process of CFRP, the drilling temperature will show a certain change pattern with the different drilling positions, but the change in drilling temperature is very different from the axial force. Through the analysis of experimental data, it can be seen that the change process of drilling temperature can be divided into three stages during the internal chip removal process, as shown in Figure 7.

Stage I is the preparation process, the drill bit has not yet touched the workpiece, the temperature measured at this time is the room temperature (the room temperature in summer is about 25°C).

Stage II is the cutting process, and the *L* point is the point where the cross-edge just starts to touch the CFRP

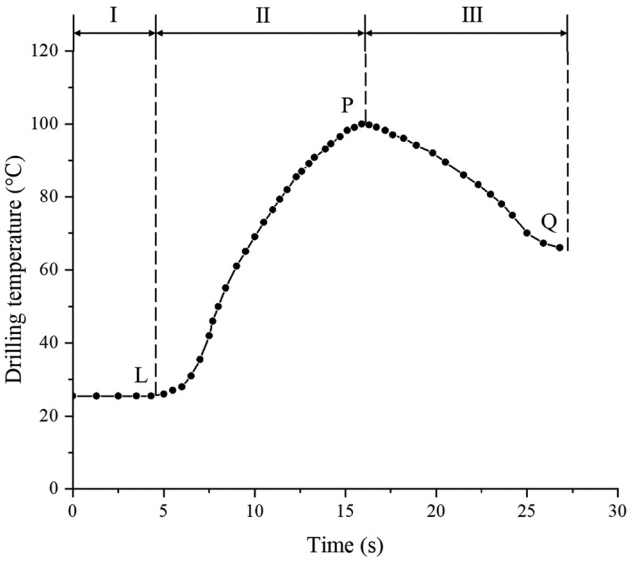

Figure 7: Drilling temperature variation curve.

Table 4: Results of orthogonal experimental data

	Factor A	Factor B	Factor C	*F*/(N)	*T*/(°C)	*W*/(μm)	CER/(μm)	VB/(μm)
1	1 (6)	1 (90)	1 (8)	90.8	94	37	42.27	223
2	1	2 (110)	2 (12)	102.75	99	33	36.56	203
3	1	3 (120)	3 (16)	101.25	102	31	34.29	186
4	1	4 (140)	4 (20)	104.5	106	30	37.15	177
5	2 (8)	1	2	98.64	99	30	33.78	201
6	2	2	1	100.35	103	39	44.38	230
7	2	3	4	105.25	106	33	34.83	223
8	2	4	3	108.78	111	37	37.35	227
9	3 (9)	1	3	100.25	100	41	45.29	235
10	3	2	4	103.5	106	30	33.31	216
11	3	3	1	105.38	108	36	37.47	216
12	3	4	2	109.83	112	35	36.43	229
13	4 (10)	1	4	94.75	109	45	57.46	252
14	4	2	3	105.68	112	34	41.65	212
15	4	3	2	106.3	114	33	40.5	210
16	4	4	1	123.6	117	40	42.87	221

Factors A, B, and C denote the drill diameter, point angle, and rear angle, respectively, F denotes the axial force, T denotes the drilling temperature, W denotes the tool chisel edge width, CER denotes the rounded cutting edge radius, and VB denotes the rear tool flank wear land width.

workpiece, *i.e.*, the beginning of drilling. At the beginning of drilling, the abrasive action between the cutting edge and the workpiece material generates drilling heat, and as the main cutting edge cuts into the workpiece, the rear face of the main cutting edge starts to rub against the machined surface. As the drilling process is semi-closed, and the thermal conductivity of CFRP material is low, the heat transferred to the surrounding environment is less, which leads to the accumulation of drilling heat, and it is mainly concentrated on the cutting edge. Therefore, the drilling temperature continues to rise until the transverse and the main cutting edges are completely drilled out of the CFRP workpiece, *i.e.*, when the drilling temperature reaches the maximum value at *P* point.

Stage III is the receding stage after the drilling is completed. At this stage, because the heat in the hole does not dissipate easily, the temperature also drops slowly, and therefore requires some time before room temperature is reached.

3 Study of the influence of tool parameters on wear conditions

During CFRP machining, the magnitude of axial force will have a direct impact on the tool wear, which will further affect the hole-machining quality and hole wall surface quality. The study of tool wear mechanism and failure form has certain research significance to improve the tool machining performance and hole-machining quality. Therefore, based on the experimental data above, this study further investigates the influence law of tool parameters on tool wear situation.

3.1 Study of the effect of drill parameters on the chisel edge width

The extreme difference method [22] was used to analyze the experimental data of CFRP drilling and machining by calculating K_{ij} (the sum of experimental values at level j of each factor) and k_{ij} (the mean of the sum of experimental values at level j of each factor), and the extreme difference R_i, which indicates the maximum difference of the mean index under the same factor. The larger the value of R_i, the more important this influencing factor is, the greater the variation in the level of this factor, and the greater the impact on experimental results [23]. R_i is derived from Equation (1).

$$R_i = \max(k_{ij}) - \min(k_{ij}). \tag{1}$$

Based on the experimental data in Table 4 and Equation (1), K_{ij}, k_{ij}, and R_i of the chisel edge width were calculated, as shown in Table 5.

From the data in Table 5, it can be seen that $R_A(W)$ = 8.25 μm, $R_B(W)$ = 8 μm, $R_C(W)$ = 5.25 μm, and $R_C(W) < R_B(W) < R_A(W)$. The chisel edge width is most significantly influenced by the drill diameter, second most influenced by the drill point angle, and the rear angle has the least influence on it, where A1-B3-C2 is the optimal level of chisel edge width. Therefore, in the case of already given machining parameters, if it is necessary to obtain a reasonable chisel edge width, the influence of the drill diameter size on the chisel edge width is given priority when selecting the tool parameters.

3.1.1 Study on the effect of drill diameter on the chisel edge width

According to the experimental data in Table 5, it can be seen that $k_{A1}(W)$ = 32.75 μm, $k_{A2}(W)$ = 34.75 μm, $k_{A3}(W)$ = 35.5 μm, and $k_{A4}(W)$ = 41 μm are not equal to each other, and $k_{A4}(W) > k_{A3}(W) > k_{A2}(W) > k_{A1}(W)$, then it indicates that changing the drill diameter size will cause the change in the chisel edge width, where A1 is the A factor of the superior level.

According to the experimental data in Table 5, the tool chisel edge width curves were plotted for different drill diameters, as shown in Figure 8.

As can be seen from Figure 8, the average and maximum chisel edge widths show an increasing trend with the increase in drill diameter, and the fluctuation of chisel edge width is the largest when the drill diameter is 9 and 10 mm. Analysis of the reason: the increase in the drill diameter and the increase in the chisel edge length lead to a larger contact area between the chisel edge and the workpiece and the chip, which makes the grinding action between the tool, the workpiece, and the chip more intense and therefore, accelerates the wear of the chisel edge.

Table 5: Data analysis of chisel edge width

	K_{i1}	K_{i2}	K_{i3}	K_{i4}	k_{i1}	k_{i2}	k_{i3}	k_{i4}	R_i
A	131	139	142	164	32.75	34.75	35.5	41	8.25
B	165	136	133	142	41.25	34	33.25	35.5	8
C	152	131	143	151	38	32.75	35.75	37.5	5.25

The primary and secondary factors affecting the chisel edge width: Drill diameter (A) > Drilling angle (B) > Rear angle (C).

3.1.2 Effect of drill point angle on the chisel edge width

According to the experimental data in Table 5, it can be seen that $k_{B1}(W)$ = 41.25 μm, $k_{B2}(W)$ = 34 μm, $k_{B3}(W)$ = 33.25 μm, and $k_{B4}(W)$ = 35.5 μm are not equal to each other, and $k_{B1}(W) > k_{B4}(W) > k_{B2}(W) > k_{B3}(W)$, then it means that changing the size of the drill point angle will cause the change in the chisel edge width, where B3 is the B factor of the superior level.

According to the experimental data in Table 5, the graphs of the chisel edge widths at different drill point angles are plotted as shown in Figure 9.

As seen in Figure 9 both the average and maximum chisel edge widths show a trend of decreasing and then increasing with the increase in the drill point angle, and the fluctuation of the average chisel edge width between 110° and 120° is less than 1 μm. Analysis: During the machining process, the size of the drill point angle will not only have an effect on the cutting force, but also on the chip removal of the drill, which will affect the tool wear and life. If the drill point angle is too small, the gradient of cutting speed on each point of the cutting edge will increase, while the cutting width will increase and the thickness will decrease, so that the force and heat generated by the drilling process are gathered on the cutting edge, and the chip removal effect is not good, resulting in the hard point particles of chips causing wear of the tool; if the drill point angle is too large, it will also accelerate the wear of the tool. Therefore, the general choice of the size of the drill point angle is about 120°.

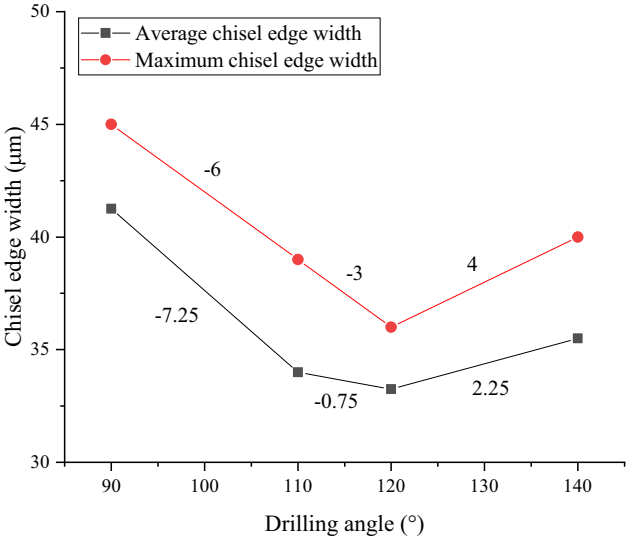

Figure 9: Chisel width at different drill point angles.

3.1.3 Influence of rear angle on chisel edge width

According to the experimental data in Table 5, it can be seen that $k_{C1}(W)$ = 38 μm, $k_{C2}(W)$ = 32.75 μm, $k_{C3}(W)$ = 35.75 μm, and $k_{C4}(W)$ = 37.5 μm are not equal to each other, and $k_{C1}(W) > k_{C4}(W) > k_{C3}(W) > k_{C2}(W)$, which means that changing the rear angle size will cause the change in the chisel edge width, where C2 is the C factor of superior level.

According to the experimental data in Table 5, the curves of the chisel edge width at different rear angles are plotted as shown in Figure 10.

As can be seen from Figure 10, the average and maximum chisel edge widths show a trend of decreasing and then increasing with the increase in the rear angle, and the overall change in the maximum chisel edge width fluctuates between 4 and 6 μm, indicating that the change in the rear angle size has a greater influence on the maximum chisel edge width. Analysis of the reason: the smaller the rear angle, the more intense the friction between the tool-

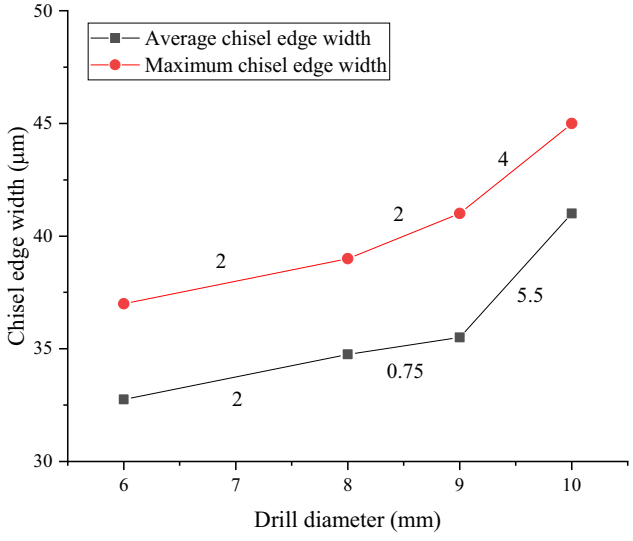

Figure 8: Chisel edge width at different drill diameters.

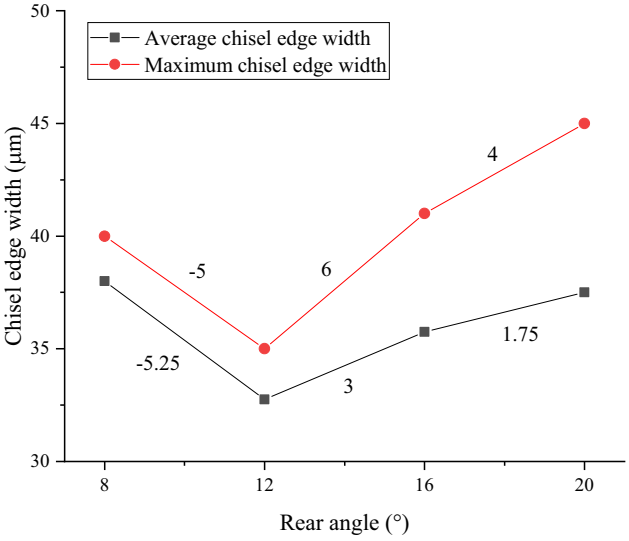

Figure 10: Chisel edge width at different rear angles.

workpiece, so the greater the amount of wear caused by hard point wear, therefore, the greater the abrasive effect between the chip and the chisel edge, resulting in increased wear. When the rear angle is too large, the radius of the cutting edge arc becomes small, making the drill especially sharp, which in turn leads to faster wear rate.

3.2 Influence of drill parameters on the rounded CER

Based on the experimental data in Table 4 and equation (1), K_{ij}, k_{ij}, and R_i of the drilling axial force are calculated, as shown in Table 6.

From the data in Table 6, it can be seen that R_A(CER) = 14.05 μm, R_B(CER) = 7.94 μm, and R_C(CER) = 4.93 μm, and R_C(CER) < R_B(CER) < R_A(CER), that is, the rounded CER is most significantly influenced by the diameter of the drill bit, followed by the drill point angle, and the rear angle has the least influence on it, where A1B3C2 is the optimal level of the rounded CER. Therefore, if a reasonable rounded CER is required for a given machining parameter, the influence of the drill diameter on the radius of the cutting edge is given priority when selecting the tool parameters.

3.2.1 Effect of drill diameter on the rounded CER

According to the experimental data in Table 6, k_{A1}(CER) = 34.57 μm, k_{A2}(CER) = 37.59 μm, k_{A3}(CER) = 38.13 μm, and k_{A4}(CER) = 48.62 μm, which are not equal to each other. k_{A4}(CER) > k_{A3}(CER) > k_{A2}(CER) > k_{A1}(CER), meaning that changing the drill diameter size causes a change in the rounded CES, where A1 is the superior level of the A factor.

According to the experimental data in Table 6, the curves of the rounded CER at different drill diameters were plotted as shown in Figure 11.

As can be seen from the figure, the average and maximum rounded CER increase with the increase in the drill diameter, and the rounded CER in the drill diameter of 9 and 10 mm change fluctuation value is greater than 10 μm, the change trend is more obvious. Analysis of the reason: When the diameter of the drill bit increases, the linear speed will become larger, and the rotation speed of the drill bit will also increase, making the friction speed between the tool and the hole wall faster, leading to the deterioration of the processing conditions at the corner of the upper outer edge of the cutting edge, further accelerating the wear rate.

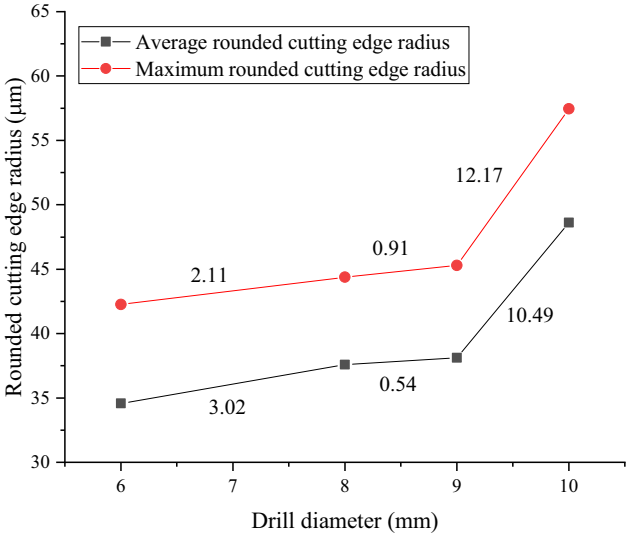

Figure 11: Rounded CER at different drill diameters.

3.2.2 Effect of drill point angle on the radius of the rounded CER

According to the experimental data in Table 6, k_{B1}(CER) = 44.7 μm, k_{B2}(CER) = 38.98 μm, k_{B3}(CER) = 36.76 μm, and k_{B2}(CER) = 38.45 μm are not equal to each other, and k_{B1}(CER) > k_{B2}(CER) > k_{B4}(CER) > k_{B3}(CER), indicating that changing the size of the drill point angle will cause a change in the rounded CES, where B3 is the superior level of the B factor.

According to the experimental data in Table 6, the curves of the rounded CER at different drilling point angles were plotted as shown in Figure 12.

Table 6: Rounded CER data analysis

	K_{i1}	K_{i2}	K_{i3}	K_{i4}	k_{i1}	k_{i2}	k_{i3}	k_{i4}	R_i
A	150.27	150.34	152.5	182.48	34.57	37.59	38.13	48.62	14.05
B	178.8	155.9	147.02	153.8	44.7	38.98	36.76	38.45	7.94
C	166.99	147.27	158.58	162.75	41.75	36.82	39.65	40.69	4.93

Primary and secondary factors affecting the rounded cutting edge radius: Drill diameter (A) > Drilling angle (B) > Rear angle (C).

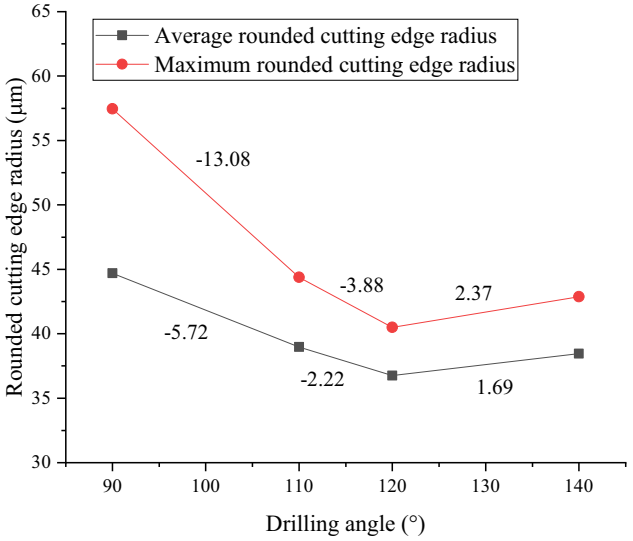

Figure 12: Round CER at different drill point angles.

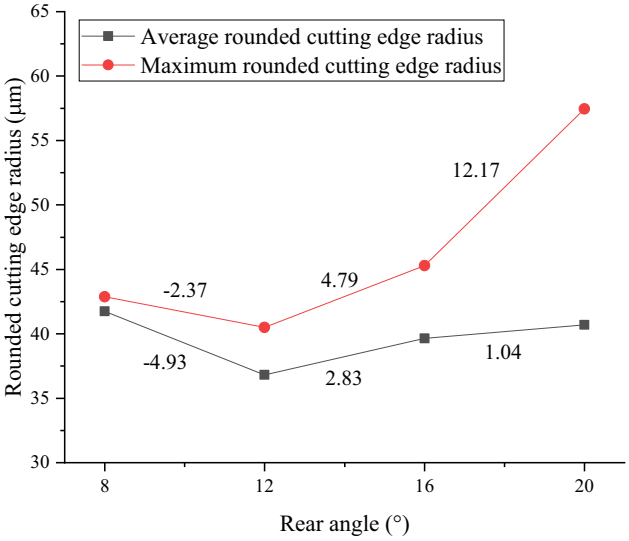

Figure 13: Round CER at different rear angles.

As can be seen from Figure 12, the average and maximum round CER show a trend of decreasing and then increasing with the increase in the drilling point angle, and the round CER fluctuates relatively more when the drilling point angle is 90° and 110°. Analysis of the reasons: the drill point angle is too large, resulting in the reduction in the tool entity at the outer edge corner, the cutting edge of the drill becomes thinner, making the heat dissipation of the tool in the process worse, which will cause accelerated wear of the drill; and the drill point angle is too small, the heat and force generated by the cutting process are gathered on the cutting edge, which will also lead to faster tool wear.

3.2.3 Effect of rear angle on the round CES

According to the experimental data in Table 6, k_{C1}(CER) = 41.75 μm, k_{C2}(CER) = 36.82 μm, k_{C3}(CER) = 39.65 μm, and k_{C4}(CER) = 40.69 μm are not equal to each other, and k_{C1}(CER) > k_{C4}(CER) > k_{C3}(CER) > k_{C2}(CER), indicating that changing the rear angle size will cause a change in the round CES, where C2 is the superior level of the C factor.

According to the experimental data in Table 6, the curves of the round CES at different rear angles are plotted as shown in Figure 13.

As can be seen from Figure 13, both the average and maximum round CER both show a trend of decreasing and then increasing with the increase in the rear angle; at the rear angle of 16° and 20°, the fluctuation value of the maximum round CER is 12.17 μm, which is the largest change at this time, while the fluctuation value of the average round CER is the smallest. Analysis of the reason: changing the rear angle of the drill will cause changes in the wedge angle, cutting edge strength, and life of the tool. Smaller rear angle and better cutting edge rigidity will significantly accelerate the wear rate, while the larger rear angle will weaken the cutting edge and the cutting edge strength of the drill, reduce the heat dissipation performance, making the drill cutting edge prone to chipping, so the drill cutting edge blunt radius value of 12° rear angle is the smallest.

3.3 Influence of drill parameters on the width of flank wear land

Based on the experimental data in Table 4 and equation (1), K_{ij}, k_{ij}, and R_i of the drilling axial force are calculated, as shown in Table 7.

According to the data in Table 7, it can be seen that R_A(VB) = 28.5 μm, R_B(VB) = 17 μm, and R_C(VB) = 9.75 μm, and R_C(VB) < R_B(VB) < R_A(VB), *i.e.*, the width of flank wear land is most significantly influenced by the diameter of the drill bit, followed by the drill point angle, and the rear angle has the least influence on it, where A1B3C2 is the optimal level of the width of the flank wear land. Therefore, if a reasonable width of the flank wear land is required for a given

Table 7: Analysis of width of flank wear land data

	K_{i1}	K_{i2}	K_{i3}	K_{i4}	k_{i1}	k_{i2}	k_{i3}	k_{i4}	R_i
A	789	886	896	903	197.25	220.25	224	225.75	28.5
B	911	861	843	854	227.75	215.25	210.75	213.5	17
C	890	851	860	868	222.5	212.75	215	217	9.75

Primary and secondary factors affecting the width of the flank wear land: Drill diameter (A) > Drilling angle (B) > Rear angle (C).

machining parameter, the influence of the drill diameter on the width of the flank wear land is given priority when selecting the tool parameters.

3.3.1 Effect of drill diameter on the width of the flank wear land

According to the experimental data in Table 7, it can be seen that k_{A1}(VB) = 197.25 μm, k_{A2}(VB) = 220.25 μm, k_{A3}(VB) = 224 μm, and k_{A4}(VB) = 225.75 μm are not equal to each other, and $k_{A4} > k_{A3} > k_{A2} > k_{A1}$, indicating that changing the drill diameter will cause a change in the width of the flank wear land, where A1 is the A factor of superior level.

According to the experimental data in Table 7, the curves of the width of the flank wear land under different drill diameters are plotted, as shown in Figure 14.

As can be seen from Figure 14, the average and maximum width of the flank wear land increases with the increase in the drill diameter; when the drill diameter is 6 and 8 mm, the fluctuation value of the average width of the flank wear land is 23 μm, which is the largest change, while the fluctuation value of the maximum width of the flank wear land is the largest when the drill diameter is 9 and 10 mm. Analysis of the reason: the diameter of the drill increases, the cutting area of the cutting edge becomes larger, and the squeezing pressure and contact area between the drill and the workpiece also become larger, which makes the tool wear intensify and the axial force of drilling increases.

3.3.2 Effect of drill point angle on the width of the flank wear land

According to the experimental data in Table 7, k_{B1}(VB) = 227.75 mm, k_{B2}(VB) = 215.25 mm, k_{B3}(VB) = 210.75 mm, and k_{B4}(VB) = 213.5 mm are not equal to each other, and k_{B1}(VB) > k_{B2}(VB) > k_{B4}(VB) > k_{B3}(VB), indicating that changing the size of the drill point angle causes the width of the flank wear land change, where B3 is the superior level of the B factor.

According to the experimental data in Table 7, the line graph of the flank wear land width at different drill diameters is plotted as shown in Figure 15.

As can be seen from Figure 15, the average and maximum width of the flank wear land both show a trend of first decreasing and then increasing with the increase in the drilling point angle, and the fluctuation value of the flank wear land width change is larger when the drilling point angle is 90° and 110°. Analysis of the reason: Under the same processing conditions, when the drill point angle increases, the front angle of the cutting edge of the drill will become larger, making the friction between the cutting edge of the drill and the workpiece significantly reduced, the drilling heat will also become smaller, which is conducive to reducing the wear of tool flank. However, when the drill point angle is too large, the cutting edge of the drill becomes thinner, resulting in a smaller tool volume for heat dissipation, and the increase in drilling heat during processing will cause accelerated wear of the drill.

3.3.3 Effect of rear angle on the width of the flank wear land

According to the experimental data in Table 7, k_{C1}(VB) = 222.5 μm, k_{C2}(VB) = 212.75 μm, k_{C3}(VB) = 215 μm, and k_{C4}(VB) = 217 μm are not equal to each other, and k_{C1}(VB) > k_{C4}(VB) > k_{C3}(VB) > k_{C2}(VB), indicate that changing the rear angle

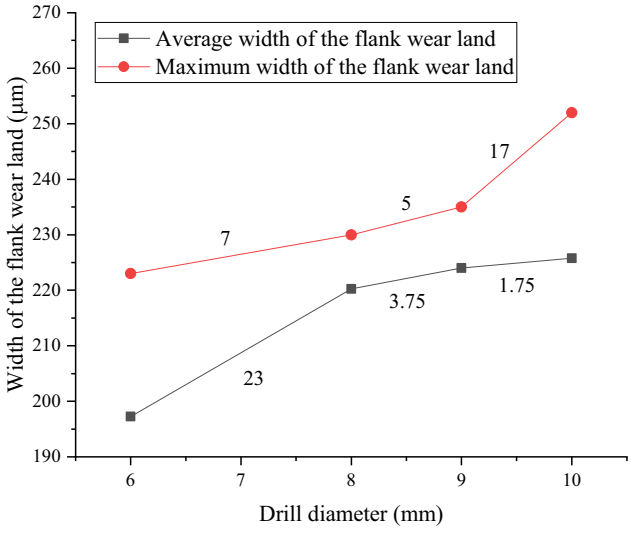

Figure 14: Width of the flank wear land at different drill diameters.

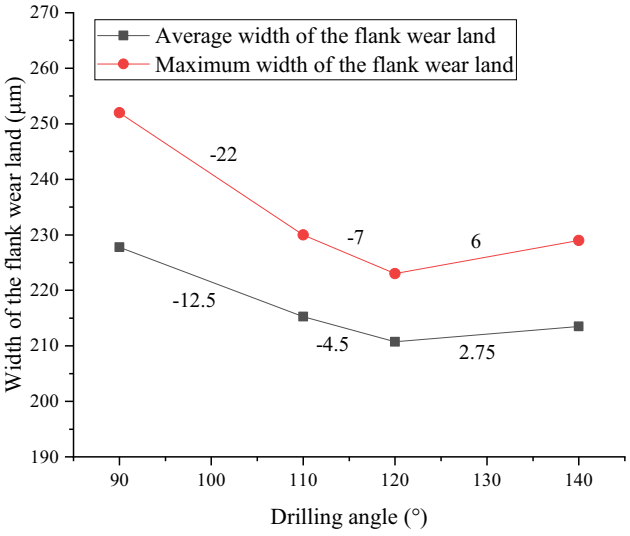

Figure 15: Width of the flank wear land at different drill point angles.

causes the change in the width of the wear zone of the rear tool face, where C2 is the superior level of C factor.

According to the experimental data in Table 7, the line graph of the width of the flank wear land at different rear angles is drawn, as shown in Figure 16.

As can be seen from Figure 16, both the average and maximum flank wear land width show a trend of decreasing and then increasing with the increase in the rear angle. Analysis of the reason: the rear angle of the drill can reduce the friction between the tool flank and the processing surface, increasing the rear angle can reduce the tool-workpiece surface friction, but also will aggravate the deterioration of the cutting edge of the tool heat dissipation conditions, making the drilling temperature rise, thus intensifying the tool wear. The smaller the rear angle, the larger the angular surface formed by the tool flank wear, and the greater the friction between the tool flank-machining surface, resulting in greater wear caused by hard point wear. Therefore, as the rear angle increases, the width of the flank wear land decreases and then increases.

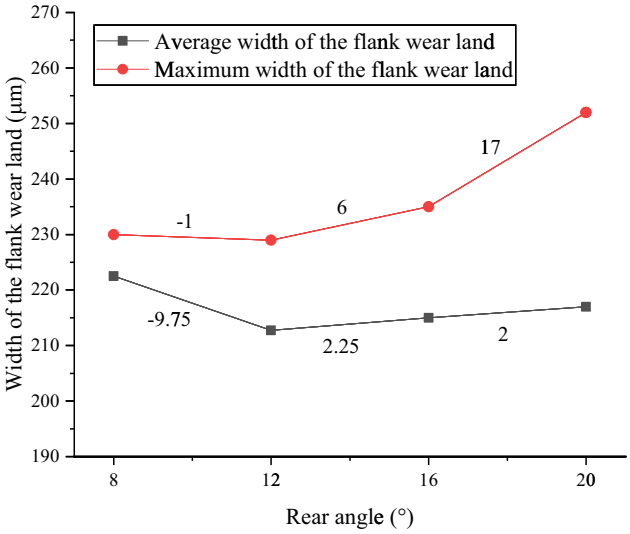

Figure 16: Width of the flank wear land at different rear angles.

4 Study on the wear law of internal chip removal drill bits

In the process of drilling and processing CFRP, the wear of the drill bit will shorten the service life of the tool and also induce processing defects, which will affect the quality of hole-machining. Due to the special structure of the internal chip removal drill bit, the force of each part in contact with the workpiece during the cutting process is different, and the internal chip removal process can discharge the chips at the first time and take away part of the cutting heat, which can reduce the friction between the tool and the chips. Therefore, it is necessary to study the tool wear law and failure forms of internal chip removal drills. In this section, based on the optimal drill parameters derived from Section 2, the carbide twist drill under the conditions of the drill diameter of 6 mm, the drill point angle of 120°, and the rear angle of 12° is selected for the tool wear law of the internal chip removal drill and the analysis of its causes.

4.1 Methods for characterizing tool wear

During the machining process of CFRP, the contact surfaces of tool-workpiece and tool-chip are prone to hard point wear due to friction, mainly because of the fiber components in the workpiece and chip. The hard point wear is mainly characterized by the formation of striped areas or the decrease in cutting edge sharpness (increase in the cutting edge arc radius), and occurs on the rake and flank faces, but the flank face wear is more intense. Therefore, in this study, cutting edge blunting and flank face wear are used as the evaluation criteria for tool wear of internal chip drill, and the rounded CER and the flank wear land width (VB) are used to characterize the degree of cutting edge blunting and flank face wear, respectively.

In this study, the rounded CER of the tool after CFRP hole-machining was measured using an ultra-depth-of-field microscope to extract the profile data of the cutting edge, as shown in Figure 17. A new algorithm proposed by Wyen *et al.* [24] is used to calculate the rounded CER by iterative method to determine the least squares circle in the wear area of the rake and flank faces.

For the measurement of VB, the tool flank face wear measurement method proposed by Çelik *et al.* [9] was used to calculate VB by comparing the cutting edge profile before and after tool wear, as shown in Figure 18. The comprehensive evaluation of tool wear by CER and VB better reflected the real condition of tool wear in CFRP drilled hole-machining.

4.2 Comparative analysis of tool wear experiments on internal and external chip removal drill bits

In the process of drilling and machining CFRP, due to the difference in tool wear between internal chip removal machining and non-internal chip removal machining, carbide drills with the drill diameter of 6 mm, the drill point

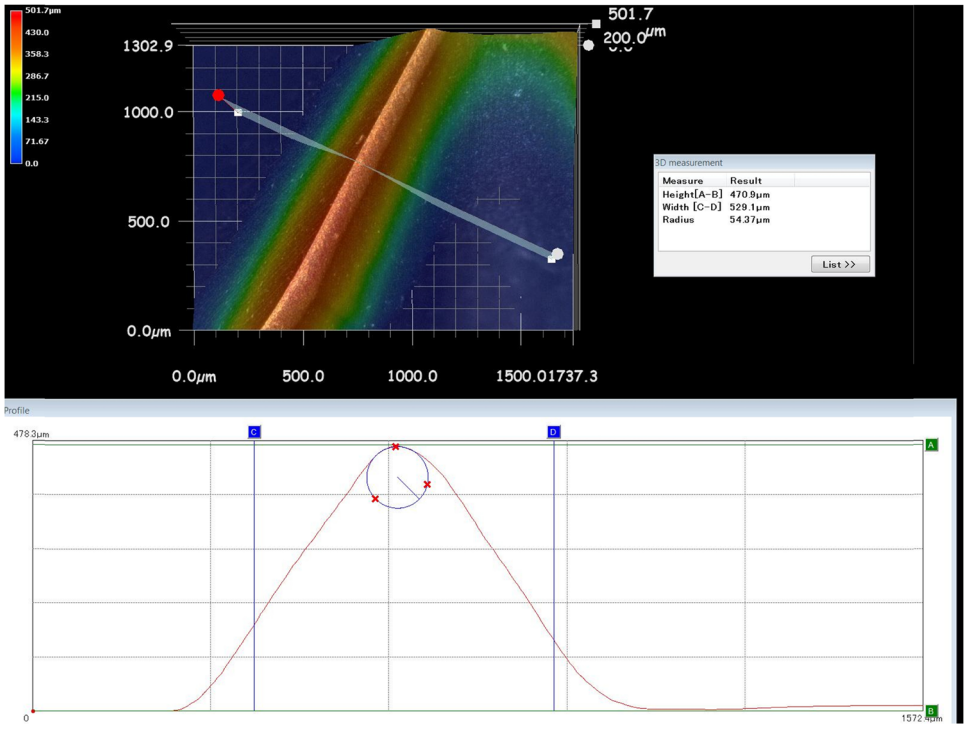

Figure 17: Cutting edge profile.

angle of 120° and the rear angle of 12° with chip removal flow channels and carbide drills without internal flow channels were selected in this section under the machining conditions of the feed rate of 20 mm/min and the spindle drilling speed of 3,000 rpm. Under the machining conditions of 3,000 rpm, the carbide drill bit with 6 mm diameter, 120° drilling angle, and 12° rear angle with chip flow channel and the carbide drill bit without internal chip flow channel were selected for internal chip flow processing and non-chip flow processing, and the comparative experimental analysis of the drilling axial force, drilling temperature, chisel width, round CER, and width of the flank wear land under the two cutting processing methods were conducted, respectively, to conclude the superiority of the internal chip flow processing method.

4.2.1 Comparative analysis of drilling axial force variation

The variation curve of drilling axial force for internal chip removal machining and non-internal chip removal machining are shown in Figure 19.

From the analysis of the experimental results, it can be seen that: (1) regardless of the use of internal chip processing or non-internal chip processing, the drilling axial force increases with the increase in the number of holes, and then decreases. (2) The drilling axial force of internal chip processing is obviously smaller than that of non-internal chip processing. This is because with the increase in the number of holes, the width of the chisel edge wear becomes larger, which makes the contact area between the workpiece and the cutting edge become larger, so the squeezing force on the workpiece increases. When internal chip removal drilling is used, the negative pressure of chip removal generates an upward suction force to offset part of the axial force, which makes the axial force of internal chip removal drilling significantly smaller than that of non-internal chip removal drilling. (3) As the number of holes

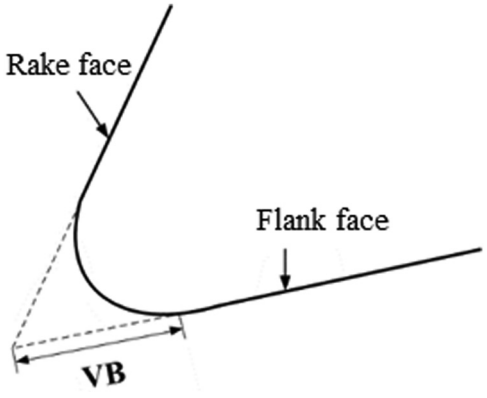

Figure 18: Width measurement of the flank wear land.

increases, the wear on the flank face increases, because the cutting edge near the flank face will be thinned, which leads to a decline in the round CER; the chip edge round CER decline, resulting in the cutting edge becoming sharp, and then the drilling force is reduced.

4.2.2 Comparative analysis of drilling temperature variation

The variation curve of drilling temperature for internal chip removal machining and non-internal chip removal machining are shown in Figure 20.

From the analysis of the experimental results, it is clear that (1) regardless of the use of internal chip processing or non-internal chip processing, the drilling temperature shows an increasing trend with the increase in the number of holes. (2) The drilling temperature of internal chip processing is obviously smaller than that of non-internal chip processing. This is due to the fact that the chip can be taken away from the cutting area at the first time when internal chip drilling is used, and part of the cutting heat is taken away, which makes the drilling temperature of internal chip processing significantly smaller than that of non-internal chip processing.

4.2.3 Comparative analysis of chisel edge width variation

The variation curves of drill chisel edge width for internal chip removal machining and non-internal chip removal machining are shown in Figure 21.

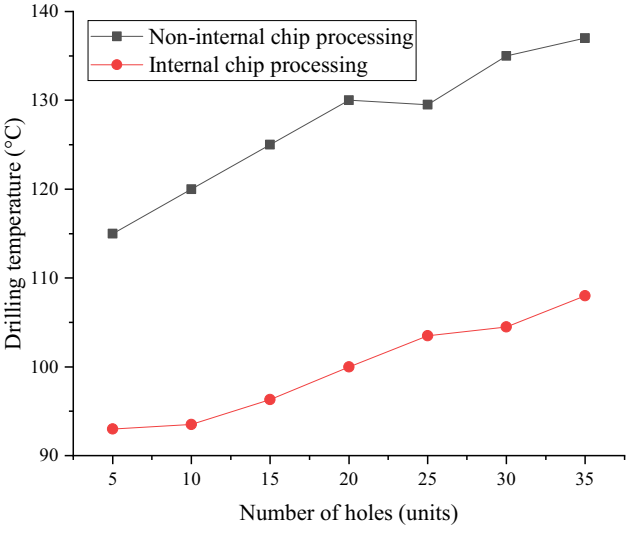

Figure 20: Drilling temperature at different number of holes.

From the analysis of the experimental results, it can be seen that (1) chisel edge width increases with the number of holes, both with and without internal chip removal; (2) the wear rate of the tool chisel edge width is almost the same for the first 25 holes with non-internal chip removal machining and internal chip removal machining; (3) after the 25th hole, the wear rate of the tool chisel edge with internal chip removal machining is slightly less than that with non-internal chip removal machining. This is due to the fact that during the drilling process, the chisel edge part is extruded from the workpiece, and with the rotating feed of the drill, the chips flow in radial and tangential directions, which makes the rate of chip discharge from the chip discharge aperture inside the drill at the chisel edge relatively slow and has no obvious effect on reducing

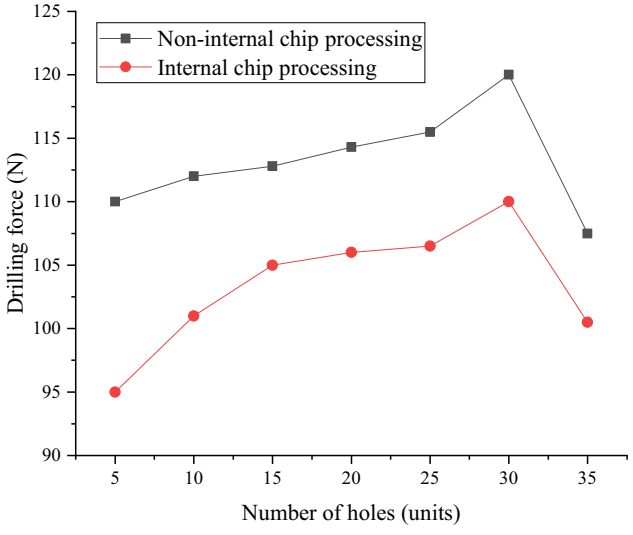

Figure 19: Drilling force at different number of holes.

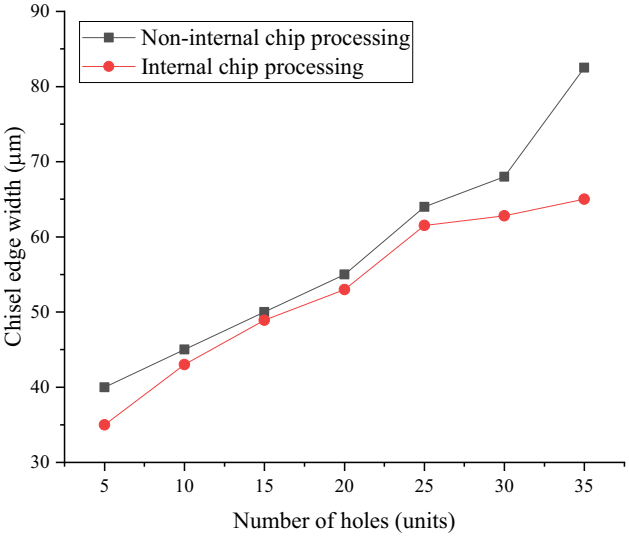

Figure 21: Chisel edge width at different number of holes.

the grinding between the chips and the tool, so there is no obvious difference in the chisel edge wear regardless of the internal chip removal process or the non-internal chip removal process.

4.2.4 Comparative analysis of rounded CER variation

The variation curve of rounded CER for internal chip removal machining and non-internal chip removal machining is shown in Figure 22.

The analysis of the experimental results shows that (1) the rounded CER increases and then decreases for both internal chip removal and non-internal chip removal machining; (2) the change in the rounded CER is smaller for internal chip removal machining than for non-internal chip removal machining when the machining parameters are certain. This is because the internal chip removal process can reduce the cutting temperature and the wear between the tool, workpiece, and chip, so the rounded CER of the internal chip removal process is smaller than that of the non-internal chip removal process; 3) The wear of the flank face increases with the number of holes. Due to wear on the flank face near the cutting edge, resulting in cutting edge thinning, and rounded CER decline.

4.2.5 Comparative analysis of flank wear land width variation

The variation curve of flank wear land width for internal chip removal machining and non-internal chip removal machining is shown in Figure 23.

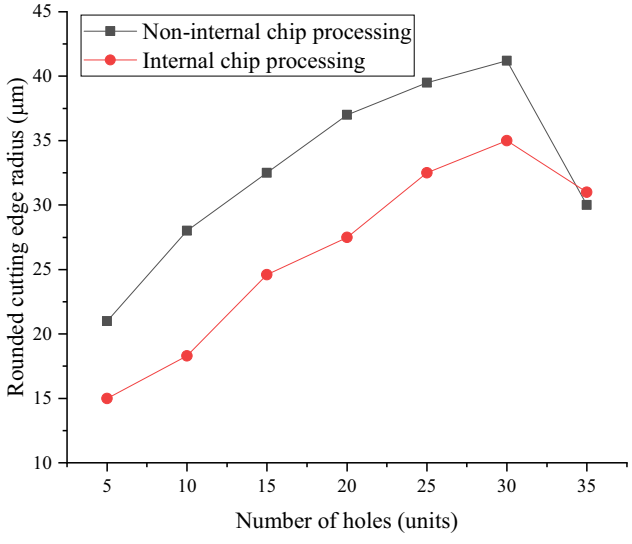

Figure 22: Rounded CER at different number of holes.

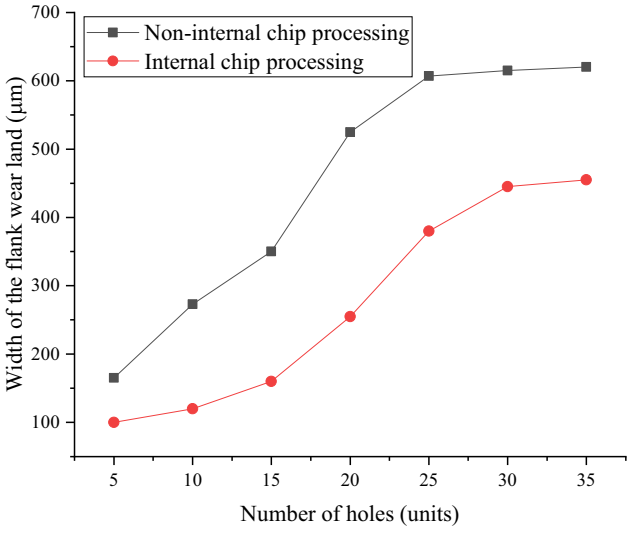

Figure 23: Width of flank wear land at different number of holes.

From the analysis of the experimental results, it can be seen that (1) the variation in the width of flank wear land shows an increasing trend for both internal chip removal and non-internal chip removal machining, and (2) the variation in the width of flank wear land is smaller when internal chip removal machining is used than that of non-internal chip removal machining when the machining parameters are certain. This is due to the fact that when internal chip removal is used, the chips at the flank face can be effectively discharged from the internal chip removal aperture of the tool at the first time, which reduces the grinding between the chips and the tool and decreases the wear rate of the cutting edge, so the width of the flank wear land of internal chip removal machining is smaller than that of non-internal chip removal machining.

5 Conclusion

1) The temperature variation curve of internal chip removal machining drilling process was plotted;
2) The influence of internal chip removal tool parameters on tool wear was studied, and it was concluded that:
   (a) The primary and secondary factors affecting the chisel edge width under given conditions: Drill diameter (A) > Drilling angle (B) > Rear angle (C):
   (b) Primary and secondary factors affecting the rounded CER under given conditions: Drill diameter (A) > Drilling angle (B) > Rear angle (C);
   (c) The primary and secondary factors affecting the width of the flank wear land under the given

conditions: Drill diameter (A) > Drilling angle (B) > Rear angle (C);

(d) It is further analyzed that at the given speed of 3,000 rpm and the feed rate of 20 mm/min, the carbide drill bit with 6 mm diameter, 120° drilling angle, and 12° rear angle has the best hole-making quality and service life.

3) Derived from the wear law of the internal chip drill:
   (a) Under the given conditions, the chisel edge width wear tends to increase with the increase in the number of holes.
   (b) Under the given conditions, the rounded CER tends to increase and then decrease with the increase in the number of holes.
   (c) Under the given conditions, the width of flank wear land tends to increase with the number of holes made.
   (d) It is concluded from further analysis that under the given conditions, the use of internal chip removal machining can effectively reduce the drilling force, drilling temperature, and tool wear generated in hole-making.

Funding information: This study has been funded by Opening Project of the Key Laboratory of Advanced Manufacturing and Intelligent Technology (Ministry of Education), Harbin University of Science and Technology KFKT202207, the National Defense Science and Technology Innovation Special Zone Fund Project (208052020162), Shenyang Aerospace University Expo project (120421007), the Key Laboratory of Fundamental Science for National Defense of Aeronautical Digital Manufacturing Process, Shenyang Aerospace University (SHSYS202106), the Key R&D program of Liaoning Province (2023JH2/101300234) and the Natural Science Foundation of Liaoning Province (2022-BS-219).

Author contributions: All authors have accepted responsibility for the entire content of this manuscript and consented to its submission to the journal, reviewed all the results and approved the final version of the manuscript. CX: conceptualization, methodology, software, investigation, formal analysis, writing – original draft, and funding acquisition; QL: conceptualization, acquisition, analysis, interpretation of data, and data curation; FL: investigation, validation, acquisition, methodology, writing – review and editing; HF: validation, project administration, and checking writing; DH: resources, validation, and visualization; NH: investigation and writing – review and editing; GW: software and funding acquisition; and YW: visualization and investigation.

Conflict of interest: Authors state no conflict of interest.

Data availablity statement: The datasets generated during and/or analysed during the current study are available from the corresponding author on reasonable request.

References

[1] Seeholzer K, krammer T, Saaeedi P, Wegener K. Analytical model for predicting tool wear in orthogonal machining of unidirectional carbon fibre reinforced polymer (CFRP). Int J Adv Manuf Technol. 2022;119:7259–89.

[2] Xu CY, Wang YW, Xu JZ, Liu XL. Calculation of negative-pressure chip in suction-type internal chip removal system and analysis of influencing factors. Int J Adv Manuf Technol. 2018;99(1a4):201–9.

[3] Laakso SVA, Agmell M, Stahl JE. The mystery of missing feed force–The effect of friction models, flank wear and ploughing on feed force in metal cutting simulations. J Manuf Process. 2018;33:268–77.

[4] Teti R. CIRP annals-manufacturing technology. Mech Compos Mater. 2002;51(2):611–34.

[5] Rawat S, Attia H. Wear mechanisms and tool life management of WC-Co drills during dry high speed drilling of woven carbon fibre composites. Wear. 2009;267(5):1022–30.

[6] Mayuet P, Gallo A, Portal A, Arroyo P, Alvarez M, Marcos M. Damaged area based study of the break-in and break-out defects in the dry drilling of carbon fiber reinforced plastics (CFRP). Procedia Eng. 2013;63:743–51.

[7] Wang X, Kwom PY, Sturtevant C, Sturtevant C, Kim D, Lantrip J. Tool wear of coated drills in drilling CFRP. J Manuf Process. 2013;15(1):127–35.

[8] Karpat Y, Deger B, Bahtiyar O. Drilling thick fabric woven CFRP laminates with double point angle drills. J Mater Process Technol. 2012;212(10):2117–27.

[9] Çelik A, Lazoglu I, Kara A, Kara F. Wear on SiAlON ceramic tools in drilling of aerospace grade CFRP composites. Wear. 2015;338-339(9):11–21.

[10] Ramirez C, Poulachon G, Rossi F, Saoubi RM. Tool wear monitoring and hole surface quality during CFRP drilling. Procedia CIRP. 2014;13:163–8.

[11] Xia T, Kaynak Y, Arvin C, Jawahir IS. Cryogenic cooling-induced process performance and surface integrity in drilling CFRP composite material. Int J Adv Manuf Technol. 2016;82(1–4):605–16.

[12] Bao YJ. Some research on drilling carbon fiber reinforced composites. DUT. 2006;2:31–59.

[13] Gao H, Liu GX, Zhang XL, Bao YJ. Study on abrasive wear characteristics of carbon fiber composites drilled with electroplated diamond tools. J Dalian Univ Techno. 2011;51(5):675–80.

[14] Zhao JS, Li ZP. Study of drilling bit wear for carbon-epoxy composites. Aerosp Mater Technol. 2006;36(2):68–70.

[15] Peng SZ, Li PN, Tang SW, Zhang S, Qiu XY. Experimental study on tool wear and machining quality in drilling carbon fiber composite. Manuf Technol Mach Tool. 2015;7:45–9.

[16] Wei LY. Experimental study on axial force and tool wear of carbon fiber composite drilling. NJUST. 2013;7:19–35.

[17] Qian BW, Liu W, Jia ZY, Fu R, Bai Y, He CL. Wear mechanism of double point angle drill bit in drilling CFRP composites. Acta Mater Compos Sin. 2017;34(4):511–29.

[18] Wang FJ, Qian BW, Cheng D, Jia ZY, Fu R, Yin JW. A new wear control method for double top Angle bit drilling CFRP. J Mech Eng. 2018;54(15):171–9.
[19] Wang FJ, Cheng D, Zhao M, Fu R. Influence of cooling air direction on tool wear and hole quality in CFRP drilling. Acta Mater Compos Sin. 2019;36(2):410–7.
[20] Yang HJ, Chen Y, Xu JH, Ladonne M, Lonfier J, Fu YC. Tool wear mechanism in low-frequency vibration-assisted drilling of CFRP/Ti stacks and its individual layer. Int J Adv Manuf Technol. 2019;104(5–8):2539–51.
[21] Li C, Xu JY, Chen M, An QL, Mansori ME, Ren R. Tool wear processes in low frequency vibration assisted drilling of CFRP/Ti6Al4V stacks with forced air-cooling. Wear. 2019;426–427:1616–23.
[22] Li ZX, Du SK. Experimental optimization design and statistical analysis. Shanghai: Science Press; 2010. p. 87–8.
[23] Xue GB. Study on the axial force and hole quality in the drilling process of CFRP. TUT. 2017;17:21–8.
[24] Wyen CF, Knapp W, Wegener K A new method for the characterisation of rounded cutting edges. Int J Adv Manuf Technol. 2012;59(9–12):899–914.